

Transport properties, upper critical field and anisotropy of $\text{Ba}(\text{Fe}_{0.75}\text{Ru}_{0.25})_2\text{As}_2$ single crystals

Jie Xing¹, Bing Shen², Bin Zeng², Jianzhong Liu¹, Xiaxin Ding¹, Zhihe Wang¹, Huan Yang¹ and Hai-Hu Wen^{1*}

¹ Center for Superconducting Physics and Materials, National Laboratory of Solid State Microstructures and Department of Physics, Nanjing University, Nanjing 210093, China and

² National Laboratory for Superconductivity, Institute of Physics, Chinese Academy of Sciences, P.O.Box 603, Beijing 100190, China

The temperature and angle dependent resistivity of $\text{Ba}(\text{Fe}_{0.75}\text{Ru}_{0.25})_2\text{As}_2$ single crystals were measured in magnetic fields up to 14 T. The temperature dependent resistivity with the magnetic field aligned parallel to c-axis and ab-planes allow us to derive the slope of dH_{c2}^{ab}/dT and dH_{c2}^c/dT near T_c yielding an anisotropy ratio $\Gamma = dH_{c2}^{ab}/dT/dH_{c2}^c/dT \approx 2$. By scaling the curves of resistivity vs. angle measured at a fixed temperature but different magnetic fields within the framework of the anisotropic Ginzburg-Landau theory, we obtained the anisotropy in an alternative way. Again we found that the anisotropy $(m_c/m_{ab})^{1/2}$ was close to 2. This value is very similar to that in $\text{Ba}_{0.6}\text{K}_{0.4}\text{Fe}_2\text{As}_2$ (K-doped Ba122) and $\text{Ba}(\text{Fe}_{0.92}\text{Co}_{0.08})_2\text{As}_2$ (Co-doped Ba122). This suggests that the 3D warping effect of the Fermi surface in Ru-doped samples may not be stronger than that in the K-doped or Co-doped Ba122 samples, therefore the possible nodes appearing in Ru-doped samples cannot be ascribed to the 3D warping effect of the Fermi surface.

PACS numbers: 74.25.Fy, 74.25.Op, 74.70.-b

The discovery of high temperature superconductivity in the iron pnictides and chalcogenides greatly stimulates the interests in understanding the novel pairing mechanism for superconductivity. Although many experiments have been done and the results demonstrate that the iron-based superconductors belong to a family with unconventional pairing mechanism[1–5], however, the detailed pairing mechanism and gap structure remain unclear. The inelastic neutron scattering indicates a resonance peak at the momentum (π, π) , which strongly suggests that the antiferromagnetic (AF) spin fluctuation may be the media for the pairing. This picture gets partial support from the NMR measurements in which a strong diverging of the $1/T_1T$ is observed when approaching the Neel temperature[6, 7]. The superconductivity vanishes simultaneously with the missing of the divergence of $1/T_1T$ in the overdoped region, suggestive of a close relationship between superconductivity and the AF spin fluctuations. According to the tight-binding fitting to the band structures, the pairing interaction by the AF spin fluctuation has been calculated for the five orbitals. It was predicted that, although the pairing channel is mainly the S_{\pm} , while some accidental nodes may exist on part of the Fermi surfaces[8–11]. In this regard, many interesting results have been obtained. For example, in LaFePO and KFe_2As_2 , nodal gaps are inferred from the penetration depth measurements[12, 13] and thermal conductivity measurements[14]. Meanwhile in many other systems, full gaps, sometime with a strong gap anisotropy were discovered[15–17]. Recently, another interesting system, namely, $\text{Ba}(\text{Fe}_{1-x}\text{Ru}_x)_2\text{As}_2$ has received intensive investigations[18–21]. Studies by thermal conductivity on $\text{Ba}(\text{Fe}_{1-x}\text{Ru}_x)_2\text{As}_2$ [22] revealed that nodal superconducting gap may exist in this material. Angle-resolved photoemission spectroscopy (ARPES) indicates that the band structure seems not changing too much when crossing the wide un-

derdoped region, leading to the great concern about the nesting effect as the pairing driven force[23]. For a gap with the structure of $\cos k_x \cdot \cos k_y$ or $\cos k_x + \cos k_y$ (the two main gap functions in the iron-based superconductors), the strong warping effect of the Fermi surfaces may lead to an intersect of the zero-gap line and the 3D fermi surface, resulting in horizontal nodal lines[17, 24, 25]. If the possible nodal gaps are induced by the strong warping effect of the 3D Fermi surface, the anisotropy measured by $\Gamma = H_{c2}^{ab}/H_{c2}^c$ should be very different in the present system compared with other optimally doped 122 systems, such as $\text{Ba}_{0.6}\text{K}_{0.4}\text{Fe}_2\text{As}_2$ (K-doped Ba122) and $\text{Ba}(\text{Fe}_{0.92}\text{Co}_{0.08})_2\text{As}_2$ (Co-doped Ba122) in which no trace of large horizontal nodal lines is discovered. In this paper, we present the temperature and angle dependent resistivity in $\text{Ba}(\text{Fe}_{0.75}\text{Ru}_{0.25})_2\text{As}_2$ single crystals in different magnetic fields. Our results indicate that the electronic anisotropy is quite similar among the three systems, K-doped, Co-doped and Ru-doped Ba122.

The single crystals of $\text{Ba}(\text{Fe}_{0.75}\text{Ru}_{0.25})_2\text{As}_2$ were grown with the self-flux method[26, 27]. The precursor materials FeAs and RuAs were made from Fe powder (99.9%, Alfa Aesar), As flakes (99.9%, Alfa Aesar) and Ru filaments (99.9%, Alfa Aesar). These starting materials were weighed and mixed in the glove box filled with Ar gas (the oxygen and water content below 0.1 PPM) and heated to 700 °C for 24 hours. Then the Ba (99.9%, Alfa Aesar), FeAs and RuAs were weighed according to the ratio Ba:Fe:Ru:As = 1:3:1:4 and mixed well, put in a quartz tube which is sealed in an iron tube and annealed at about 1200 °C for 20 minutes. In order to protect the iron tube from being oxidized, an additional quartz tube is shielded outside the iron tube. A slow cooling down with a rate of 2 °C/hour of the iron-tube was taken from 1200 °C to 1010 °C, and then the power of the furnace was turned off. The crystals with black and shiny surface and about 3 mm × 3 mm in dimensions are cleaved from the grown-mixture. The XRD diffraction patterns show only the (00l) peaks with a very narrow full-width at the half-maximum (FWHM). The true composition of the single crystal was checked with the

*Electronic address: hhwen@nju.edu.cn

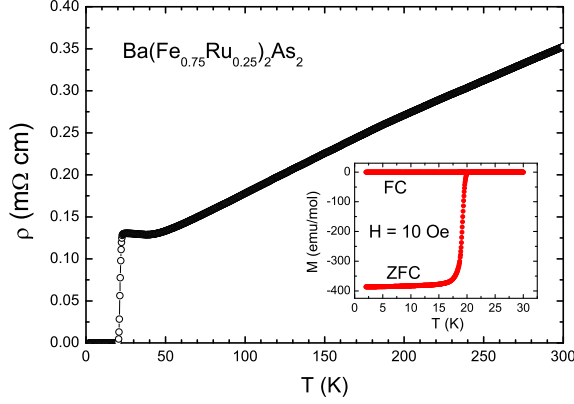


FIG. 1: (color online) Main panel: The temperature dependence of resistivity for the $\text{Ba}(\text{Fe}_{0.75}\text{Ru}_{0.25})_2\text{As}_2$ single crystal in zero field. Inset: The temperature dependent DC magnetization of the sample.

Energy-dispersive X-ray spectroscopy (EDX) and found to be close to the nominal one. The resistivity measurements were taken on a Quantum Design physical property measurement system (QD, PPMS) with the magnetic fields up to 14 T. The angle dependent resistivity was measured with a horizontal rotator (HR) on PPMS. The temperature dependence of magnetization was measured by a SQUID-VSM (Quantum Design) in the zero-field-cooling mode (ZFC) and the field-cooling mode (FC). The temperature dependence of resistivity and magnetization are shown in Fig. 1. The onset of superconducting transition is found to be 22 K in the $\rho(T)$ curve, with a transition width $\Delta T_c \approx 1.6$ K (10% to 90% ρ_n). The little upturn of the resistivity just above T_c suggests that our sample resides at a slight underdoping level. The DC magnetization measured at a magnetic field of 10 Oe exhibits a sharp transition and shows a full volume of Meissner screening at 2 K.

Fig. 2 shows the temperature dependence of the resistivity measured in different magnetic fields for both $H \parallel ab$ and $H \parallel c$. One can see a systematic suppression of the transition temperature in the magnetic fields. As seen in other iron-based superconductors, the T_c is suppressed more rapidly for $H \parallel c$ than for $H \parallel ab$, indicating a higher upper critical field H_{c2} for $H \parallel ab$. This parallel shift of the resistive curves under magnetic fields suggest that the superconducting fluctuation is weak in this sample.

Taking the criterions of 90% ρ_n and 1% ρ_n , we determined the value of the upper critical field H_{c2} and the irreversible field H_{irr} respectively, the results are shown in Fig. 3. The $H_{c2}(T)$ curves show a roughly linear T -dependent behavior, yielding the slopes $-dH_{c2}^c/dT_c|_{T_c} = 3.55$ T/K for $H \parallel ab$ and $-dH_{c2}^c/dT_c|_{T_c} = 1.82$ T/K for $H \parallel c$. These slopes are generally smaller than those in $\text{Ba}_{0.6}\text{K}_{0.4}\text{Fe}_2\text{As}_2$ and $\text{Ba}(\text{Fe}_{0.92}\text{Co}_{0.08})_2\text{As}_2$, suggesting a lower upper critical field in the Ru-doped samples. According to the Werthamer-Helfand-Hohenberg (WHH)[28] formula $H_{c2} = -0.69(dH_{c2}/dT)|_{T_c}T_c$, the calculated upper critical fields are $H_{c2}^c(0) = 54.3$ T and $H_{c2}^c(0) = 27.8$ T. The anisotropy ratio determined here is

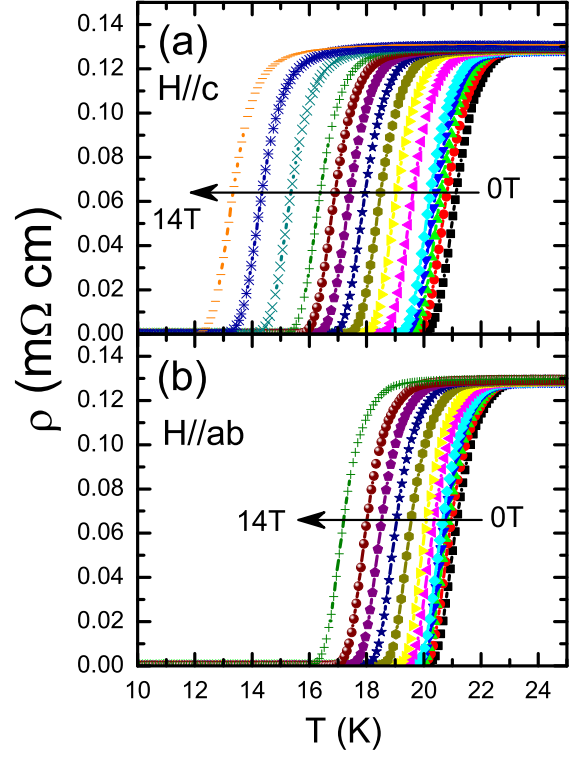


FIG. 2: (color online) (a) The in-plane resistivity of $\text{Ba}(\text{Fe}_{0.75}\text{Ru}_{0.25})_2\text{As}_2$ single crystal in different magnetic fields $H = 0, 0.25, 0.5, 0.75, 1, 2, 3, 4, 5, 6, 7, 8, 10, 12, 14$ T for $H \parallel c$. (b) The in-plane resistivity of $\text{Ba}(\text{Fe}_{0.75}\text{Ru}_{0.25})_2\text{As}_2$ single crystal in different magnetic fields $H = 0, 0.25, 0.5, 0.75, 1, 2, 3, 4, 5, 7, 9, 11, 14$ T for $H \parallel ab$.

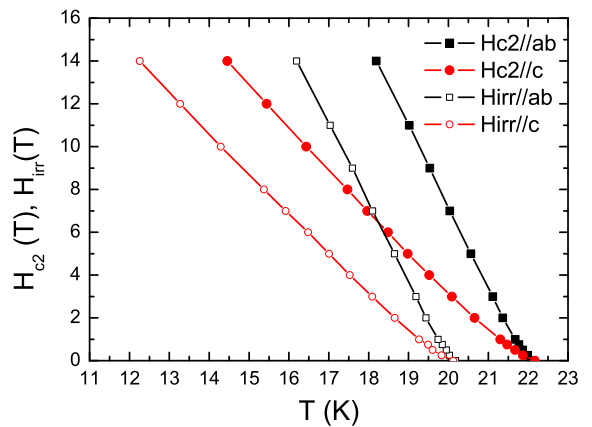


FIG. 3: (color online) The upper critical field and the irreversible field of $\text{Ba}(\text{Fe}_{0.75}\text{Ru}_{0.25})_2\text{As}_2$ single crystal for $H \parallel c$ and $H \parallel ab$, respectively. The criterions for determining H_{c2} and H_{irr} are 90% ρ_n and 1% ρ_n , respectively.

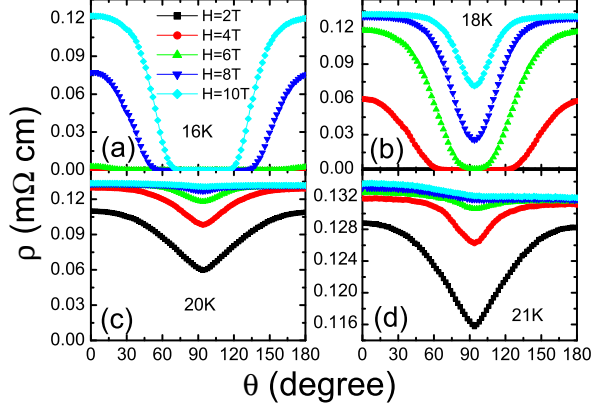


FIG. 4: (color online) Angular dependence of resistivity at (a) 16 K, (b) 18 K, (c) 20 K and (d) 21 K in $H = 2, 4, 6, 8, 10$ T for the $\text{Ba}(\text{Fe}_{0.75}\text{Ru}_{0.25})_2\text{As}_2$ single crystal.

$\Gamma = H_{c2}^{ab}(0)/H_{c2}^c(0) = 54.3/27.8 = 1.95$. The values of H_{c2} in the present system is relatively small compared to others in the family of iron-based superconductors, but the Γ is quite similar among all the Ba122 systems (see below)[25]. As we know, the Pauli limit for singlet pairing is determined by $H_{c2}(0)/k_B T_c = 1.84$ T/K[29] when the spin-orbital coupling is weak, therefore the upper critical fields may be limited by the Pauli limit $H_{c2}^{\text{Pauli}} \approx 36$ T at low temperatures. It has been pointed out that the WHH formula, proposed for conventional s-wave superconductor, may not apply for the iron-based superconductors, which have been proved to be governed by an unconventional superconducting mechanism[30]. However, the value of $-dH_{c2}^{ab}/dT$ is proportional to $(m_{ab} \times m_c)^{1/2}$, while $-dH_{c2}^c/dT \propto m_{ab}$, therefore the ratio determined by $dH_{c2}^{ab}/dT|_{T_c}/dH_{c2}^c/dT|_{T_c} \approx 1.95$ is reliably telling the anisotropy of the averaged electron mass near the transition temperature. In Fig. 3 we also present the irreversibility lines $H_{irr}^{ab}(T)$ and $H_{irr}^c(T)$, taking the criterion of $1\% \rho_n$. One can see that the two lines, $H_{c2}(T)$ and $H_{irr}(T)$, are parallel to each other. The area between the lines of $H_{c2}(T)$ and $H_{irr}(T)$ is small for both cases of $H \parallel c$ and $H \parallel ab$, indicating a quite weak vortex thermal fluctuation effect. This is well associated with the small anisotropy factor $\Gamma = 1.95$.

In order to further determine the anisotropy Γ , we measured the angle-dependent resistivity of $\text{Ba}(\text{Fe}_{0.75}\text{Ru}_{0.25})_2\text{As}_2$ in different magnetic fields at several fixed temperatures. The typical results are shown in Fig. 4. The θ is the angle that encloses between the magnetic field and c-axis. During the measurements, the magnetic field is always applied perpendicular to the direction of the applied current. Therefore $\theta = 0^\circ$ and $\theta = 90^\circ$ represent the cases of $H \parallel c$ and $H \parallel ab$, respectively. According to the anisotropic Ginzburg-Landau theory, the angle dependent upper critical field is given by

$$H_{c2}^{GL}(\theta) = H_{c2}^c / \sqrt{\sin^2(\theta) + \Gamma^2 \cos^2(\theta)}. \quad (1)$$

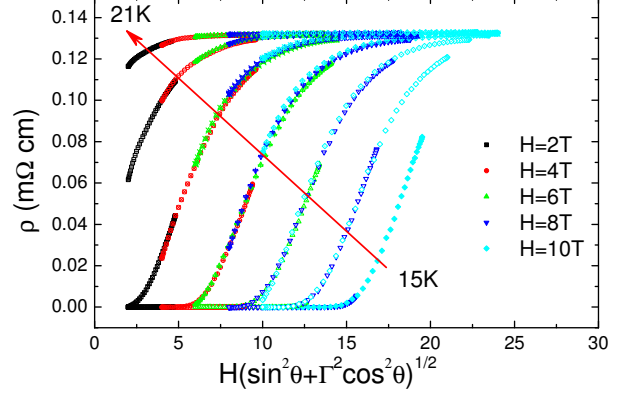


FIG. 5: (color online) Scaling of the resistivity versus $\tilde{H} = H \sqrt{\sin^2(\theta) + \Gamma^2 \cos^2(\theta)}$ at 15, 16, 17, 18, 19, 20, 21 K in different magnetic fields. For each temperature, Γ is adjusted to achieve the best scaling.

with the anisotropy

$$\Gamma = H_{c2}^{ab}/H_{c2}^c = (m_c/m_{ab})^{1/2} = \xi_{ab}/\xi_c. \quad (2)$$

It has been proposed by Blatter et al.[31] that, if we take the x-coordinate as $\tilde{H} = H \sqrt{\sin^2(\theta) + \Gamma^2 \cos^2(\theta)}$, and re-plot the data as ρ vs. \tilde{H} , the curves for different magnetic field at the same temperature will collapse into one. This scaling law can be used to determine the anisotropy factor Γ at each temperature. Fig. 5 shows the scaled results for temperatures from 15 K to 22 K. One can see a good scaling for all temperatures. And Γ is optimized for each temperature to achieve the best scaling. The value of Γ determined from the scaling is about 2, which is consistent with the value derived from the upper critical field, as discussed above. And Γ shows a temperature dependent variation. It increases monotonically from 1.95 at 15 K to 2.4 at 20 K, and then drops slightly to 2.25 at 21 K.

In Fig. 6, we show a collection of the anisotropy for the K-doped, Co-doped, Ru-doped Ba122 and RbFe_2Se_2 [32, 33]. It is found that the absolute value of Γ and its temperature dependence in the Ru-doped sample is quite similar to that of Co-doped and K-doped Ba122 samples. Regarding this similarity, it is hard to believe that the warping effect in the Ru-doped sample is much stronger than that in its counterparts Co-doped and K-doped Ba122 samples. Therefore the possible nodal gap in the Ru-doped samples may arise from other effect, instead of the strong Fermi surface warping effect. Recently, the ARPES measurements[23, 34] indicates that the Fermi surface evolves slowly, and the Fermi velocity v_F (at $k_z = \pi$) seems also weakly changed up to the optimal doping point (at around $x = 0.3$) in $\text{Ba}(\text{Fe}_{1-x}\text{Ru}_x)_2\text{As}_2$. However, towards more doping of Ru in the underdoped region, the AF state is strongly suppressed and superconductivity starts to appear at $x = 0.15$ and gets the optimized T_c at about $x = 0.30$. Clearly it is hard to understand that the superconductivity is purely induced by the effect of the Fermi surface nesting.

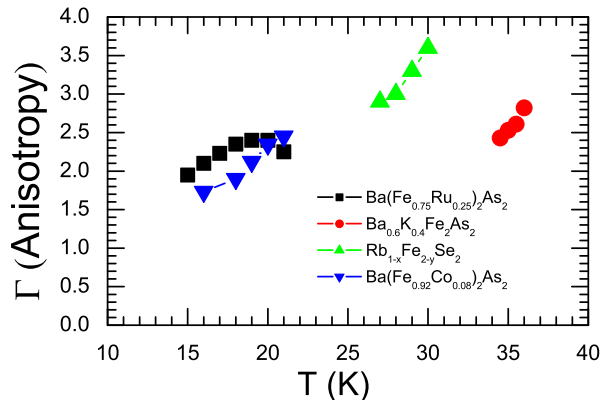


FIG. 6: (color online) Temperature dependent anisotropy Γ of $\text{Ba}(\text{Fe}_{0.75}\text{Ru}_{0.25})_2\text{As}_2$, $\text{Ba}_{0.6}\text{K}_{0.4}\text{Fe}_2\text{As}_2$, $\text{Rb}_{1-x}\text{Fe}_{2-y}\text{Se}_2$ and $\text{Ba}(\text{Fe}_{0.92}\text{Co}_{0.08})_2\text{As}_2$ single crystals.

Furthermore, it is also quite difficult to understand why the anisotropy in the three different systems are similar to each other, since Co-doped sample has larger electron Fermi surfaces, while the K-doped one has larger hole pockets, and the

Ru-doped sample is close to the case of iso-valent doping. To unravel this puzzle, it is highly desired to do further more elegant band structure calculations, and more detailed ARPES measurements.

In summary, we have measured the temperature and angle dependent resistivity for $\text{Ba}(\text{Fe}_{0.75}\text{Ru}_{0.25})_2\text{As}_2$ single crystals in magnetic fields up to 14 T for $H \parallel c$ and $H \parallel ab$. The calculated upper critical fields are $H_{c2}^{ab}(0) = 54.3$ T and $H_{c2}^c(0) = 27.8$ T, being smaller than that in other Ba122 iron-based superconductors. Interestingly, the anisotropy $\Gamma \approx 1.95$ is similar to the optimally Co-doped or K-doped Ba122. The anisotropy is also rechecked with an independent way, that is to scale the resistivity vs. angle curves measured at different magnetic fields but at a fixed temperature. Both methods yield similar anisotropy. The similar value of anisotropy found in the Co-doped, K-doped and the Ru-doped Ba122 systems suggest that the 3D warping effect of the Fermi surface may not be the cause for the appearance of the nodal gap.

Acknowledgments

This work is supported by the NSF of China (11034011/A0402), the Ministry of Science and Technology of China (973 projects: 2011CBA00102 and 2012CB821403) and PAPD.

-
- [1] I. I. Mazin, D. J. Singh, M. D. Johannes, and M. H. Du, *Phys. Rev. Lett.* **101**, 057003 (2008).
- [2] K. Kuroki, S. Onari, R. Arita, H. Usui, Y. Tanaka, H. Kontani, and H. Aoki, *Phys. Rev. Lett.* **101**, 087004 (2008).
- [3] T. Hanaguri, S. Niitaka, K. Kuroki, and H. Takagi, *Science* **328**, 474(2010).
- [4] A. D. Christianson, E. A. Goremychkin, R. Osborn, S. Rosenkranz, M. D. Lumsden, C. D. Malliakas, I. S. Todorov, H. Claus, D. Y. Chung, M. G. Kanatzidis, R. I. Bewley, and T. Guidi, *Nature* **456**, 930-932 (2008).
- [5] D. S. Inosov, J. T. Park, P. Bourges, D. L. Sun, Y. Sidis, A. Schneidewind, K. Hradil, D. Haug, C. T. Lin, B. Keimer, and V. Hinkov, *Nature Physics* **6**, 178 - 181 (2010).
- [6] F. L. Ning, K. Ahilan, T. Imai, A. S. Sefat, M. A. McGuire, B. C. Sales, D. Mandrus, P. Cheng, B. Shen, and H. -H. Wen, *Phys. Rev. Lett.* **104**, 037001 (2010).
- [7] Y. Nakai, T. Iye, S. Kitagawa, K. Ishida, H. Ikeda, S. Kasahara, H. Shishido, T. Shibauchi, Y. Matsuda, and T. Terashima, *Phys. Rev. Lett.* **105**, 107003 (2010).
- [8] V. Mishra, G. Boyd, S. Graser, T. Maier, P. J. Hirschfeld, and D. J. Scalapino, *Phys. Rev. B* **79**, 094512 (2009).
- [9] Kazuhiko Kuroki, Hidetomo Usui, Seiichiro Onari, Ryotaro Arita, Hideo Aoki, *Phys. Rev. B* **79**, 224511 (2009).
- [10] S. Graser, A. F. Kemper, T. A. Maier, H.-P. Cheng, P. J. Hirschfeld, and D. J. Scalapino, *Phys. Rev. B* **81**, 214503 (2010).
- [11] P. J. Hirschfeld, M.M. Korshunov, and I.I. Mazin, *Reports on Progress in Physics* **74**, 124508 (2011).
- [12] Clifford W. Hicks, Thomas M. Lippman, Martin E. Huber, James G. Analytis, Jiun-Haw Chu, Ann S. Erickson, Ian R. Fisher, and Kathryn A. Moler, *Phys. Rev. Lett.* **103**, 127003 (2009).
- [13] J. D. Fletcher, A. Serafin, L. Malone, J. G. Analytis, J.-H. Chu, A. S. Erickson, I. R. Fisher, and A. Carrington, *Phys. Rev. Lett.* **102**, 147001 (2009).
- [14] J. K. Dong, S. Y. Zhou, T. Y. Guan, H. Zhang, Y. F. Dai, X. Qiu, X. F. Wang, Y. He, X. H. Chen, and S. Y. Li, *Phys. Rev. Lett.* **104**, 087005 (2010).
- [15] B. Zeng, G. Mu, H. Q. Luo, T. Xiang, I. I. Mazin, H. Yang, L. Shan, C. Ren, P. C. Dai, and H. H. Wen, *Nat. Commun.* **1**, 112 (2010).
- [16] K. Hashimoto, M. Yamashita, S. Kasahara, Y. Senshu, N. Nakata, S. Tonegawa, K. Ikeda, A. Serafin, A. Carrington, T. Terashima, H. Ikeda, T. Shibauchi, and Y. Matsuda, *Phys. Rev. B* **81**, 220501(R) (2010).
- [17] Y. Zhang, Z. R. Ye, Q. Q. Ge, F. Chen, Juan Jiang, M. Xu, B. P. Xie, and D. L. Feng, accepted by *Nature Physics*, (2012).
- [18] S. Sharma, A. Bharathi, S. Chandra, R. Reddy, S. Paulraj, A. Satya, V. Sastry, A. Gupta, and C. Sundar, *Phys. Rev. B* **81**, 174512 (2010).
- [19] A. Thaler, N. Ni, A. Kracher, J. Q. Yan, S. L. Budko, and P. C. Canfield, *Phys. Rev. B* **82**, 014534 (2010).
- [20] M. G. Kim, D. K. Pratt, G. E. Rustan, W. Tian, J. L. Zarestky, A. Thaler, S. L. Budko, P. C. Canfield, R. J. McQueeney, A. Kreyssig, and A. I. Goldman, *Phys. Rev. B* **83**, 054514 (2011).
- [21] F. Rullier-Albenque, D. Colson, A. Forget, P. Thuéry, and S. Poissonnet, *Phys. Rev. B* **81**, 224503 (2010).
- [22] X. Qiu, S. Y. Zhou, H. Zhang, B. Y. Pan, X. C. Hong, Y. F. Dai, Man Jin Eom, Jun Sung Kim, Z. R. Ye, Y. Zhang, D. L. Feng, and S. Y. Li, *Phys. Rev. X* **2**, 011010 (2012).
- [23] R. S. Dhaka, Chang Liu, R. M. Fernandes, Rui Jiang, C. P. Strehlow, Takeshi Kondo, A. Thaler, Jorg Schmalian, S. L.

- Bud'ko, P. C. Canfield, Adam Kaminski, Phys. Rev. Lett. **107**, 267002 (2011).
- [24] R. T. Gordon, N. Ni, C. Martin, M. A. Tanatar, M.D. Vannette, H. Kim, G. D. Samolyuk, J. Schmalian, S. Nandi, A. Kreyssig, A. I. Goldman, J. Q. Yan, S. L. Budko, P. C. Canfield, and R. Prozorov, Phys. Rev. Lett. **102**, 127004 (2009).
- [25] J.-Ph. Reid, M. A. Tanatar, X. G. Luo, H. Shakeripour, N. Doiron-Leyraud, N. Ni, S. L. Budko, P. C. Canfield, R. Prozorov, and Louis Taillefer, Phys. Rev. B **82**, 064501 (2010).
- [26] M. J. Eom, S. W. Na, C. Hoch, R. K. Kremer, and J. S. Kim, arXiv:1109.1083 (2011).
- [27] N. Ni, M. E. Tillman, J.-Q. Yan, A. Kracher, S. T. Hannahs, S. L. Budko, and P. C. Canfield, Phys. Rev. B **78**, 214515 (2008).
- [28] N. R. Werthamer, E. Helfand, and P. C. Hohenberg, Phys. Rev. **147**, 295 (1966).
- [29] A. M. Clogston, Phys. Rev. Lett. **9**, 266 (1962).
- [30] G. Fuchs, S.-L. Drechsler, N. Kozlova, G. Behr, A. Koehler, J. Werner, K. Nenkov, C. Hess, R. Klingeler, J.E. Hamann-Borrero, A. Kondrat, M. Grobosch, M. Knupfer, J. Freudenberger, B. Buechner, and L. Schultz, Phys. Rev. Lett. **101**, 237003 (2008).
- [31] G. Blatter, V. B. Geshkenbein, and A. I. Larkin, Phys. Rev. Lett. **68**, 875 (1992).
- [32] Zhao-Sheng Wang, Hui-Qian Luo, Cong Ren, and Hai-Hu Wen, Phys. Rev. B **78**, 140501 (2008).
- [33] Chun-Hong Li, Bing Shen, Fei Han, Xiyu Zhu, and Hai-Hu Wen, Phys. Rev. B **83**, 184521 (2011).
- [34] N. Xu, T. Qian, P. Richard, Y.-B. Shi, X.-P. Wang, P. Zhang, Y.-B. Huang, Y.-M. Xu, H. Miao, G. Xu, G.-F. Xuan, W.-H. Jiao, Z.-A. Xu, G.-H. Cao, and H. Ding, arXiv:1203.4699.